Atmospheric Environment 190 (2018) 35–42

Contents lists available at ScienceDirect

Atmospheric Environment

journal homepage: www.elsevier.com/locate/atmosenv

Attribution of aerosol direct radiative forcing in China and India to emitting sectors

Meng Gao[a,*], Dongsheng Ji[b,**], Fengchao Liang[c,d], Yang Liu[d]

[a] John A. Paulson School of Engineering and Applied Sciences, Harvard University, Cambridge, MA 02138, USA
[b] State Key Laboratory of Atmospheric Boundary Layer Physics and Atmospheric Chemistry, Institute of Atmospheric Physics, Chinese Academy of Sciences, Beijing, China
[c] Department of Epidemiology, Fuwai Hospital, State Key Laboratory of Cardiovascular Disease, National Center for Cardiovascular Diseases, Chinese Academy of Medical Sciences and Peking Union Medical College, Beijing 100037, China
[d] Department of Environmental Health, Rollins School of Public Health, Emory University, Atlanta, GA 30322, USA

ARTICLE INFO

Keywords:
Aerosol radiative forcing
Climate-chemistry modeling
Emission sectors
China
India

ABSTRACT

Strict emission control measures are being implemented in China and India to improve air quality and protect human health, yet current air quality driven and sector based measures without consideration of climate effects would likely taccelerate warming. In this study, we attribute aerosol direct radiative forcing in China and India to emitting sectors using a fully online coupled meteorology-chemistry model (WRF-Chem, Weather Research and Forecasting Model coupled with Chemistry) for the entire year of 2013. Our simulations show that the observed spatial and temporal variations of aerosol concentrations and optical properties are generally reproduced by the model, although sulfate is biased low in winter due to missing aqueous/heterogeneous pathways in the model. Aerosols from all sectors result in negative direct forcing at the top of the atmosphere (TOA) in both China (-2.21 W/m^2) and India (-3.18 W/m^2), which are largely contributed by the power sector. The residential sector in both China and India largely heats the atmosphere because of its dominant contribution to black carbon emissions. In both China and India, the longwave radiative forcing (0.86 and 1.21 W/m^2 for China and India) is tiny compared to the shortwave radiative forcing (-3.07 and -4.39 W/m^2 for China and India). The seasonality of sectoral radiative forcing in China is different from that in India. These results suggest that residential sector should be targeted to achieve both air quality and climate change goals, yet the control of emissions from the power sector is very likely to accelerate warming.

1. Introduction

The Industrial Revolution that began in Britain in the 18th century and spread to other parts of the world have led to enormous economic and social benefits, but also to two important environmental problems: air pollution and climate change (Unger, 2012). Climate change and air pollution are closely connected since greenhouse gases and air pollutants originate from similar sources, and air pollution and climate change influence each other through complex interactions (Unger, 2012). Climate change mitigation is of particular importance, yet climate policy typically focuses on greenhouse gases while the role of short-lived pollutants is less appreciated (Shindell et al., 2008). The most important short-lived pollutants that influence the climate are tropospheric ozone and atmospheric aerosols including black carbon, sulfate, nitrate, and organic aerosol (Stohl et al., 2015). Similar to other long-lived greenhouse gases, ozone's contribution to radiative forcing is large and positive (Pachauri et al., 2014), and the emission reductions would be beneficial to air quality, climate and human health. Nevertheless, it is more complicated for aerosols. Anthropogenic and natural aerosols scatter and absorb radiation to alter energy balance directly, and indirectly through aerosol-cloud interactions (Pachauri et al., 2014). Although air quality driven emission reductions for aerosols may lead to substantial economic and health benefits, it may oppositely affect climate (Shindell et al., 2008). The contribution of BC to aerosol direct radiative forcing is positive and large, while the contributions of all other aerosols are negative (Pachauri et al., 2014). Thus, current air quality driven and sector based emission control measures without consideration of climate effects is likely to accelerate warming. In heavily polluted countries, such as China and India, aerosol radiative forcing can even reach tens of W/m^2 locally. Current strict aerosol pollution control measures might lead to uncertain effects on regional climate there. For example, increasing emissions of aerosol precursors

* Corresponding author.
** Corresponding author.
E-mail addresses: mgao2@seas.harvard.edu (M. Gao), jds@mail.iap.ac.cn (D. Ji).

https://doi.org/10.1016/j.atmosenv.2018.07.011
Received 28 February 2018; Received in revised form 28 June 2018; Accepted 8 July 2018
Available online 10 July 2018
1352-2310/ © 2018 Elsevier Ltd. All rights reserved.

in the Sichuan Basin, China has resulted in negative radiative forcing and surface cooling (Qian and Giorgi, 2000); the advection of the warmer air heated by BC over the Himalayas leads to a warming of about 0.6 °C in the lower and middle troposphere of that region (Ramanathan and Carmichael, 2008). Air quality control has been frequently linked to emission sectors, while there has been limited study of the contributions of different source sectors to aerosol radiative forcing, which is important to policymakers to consider the benefits of synergies between air pollution and climate change.

Previous studies have estimated the radiative forcing of the short-lived air pollutants by source regions and emission sectors (Koch et al., 2007a; b; Shindell et al., 2008; Streets et al., 2013; Unger et al., 2008; Unger et al., 2009; Unger et al., 2010; Unger et al., 2013), using the NASA GISS general circulation model (Schmidt et al., 2006). Simulations were run using a 4 × 5 horizontal resolution and some aerosol species, such as dust and nitrate, are ignored, but could play an important role in regional climate. Dang and Unger (2015) found that regional radiation budget exerted by megacities could be 10–100 times larger than global effects. Focus on regional climate effects of aerosols in heavily polluted regions is also of great importance, as different temperature tendency from global warming has been found in China and India in recent decades (Menon et al., 2002). In addition, there have been many measurement-based and modeling based estimates of shortwave radiative forcing (Yu et al., 2006), yet estimates of longwave radiative forcing are limited (Pachauri et al., 2014).

In this work, we use a regional scale chemistry-meteorology model, with sophisticated aerosol chemistry treatments (including all important aerosol species in regional and urban scale) and mesoscale meteorological parameterizations, to provide the local effects of emission sectors on radiative forcing and implications for air quality and climate mitigation efforts. Additionally, estimates of both shortwave and longwave radiative forcing are offered, and the seasonality of aerosol radiative forcing for different sectors are discussed.

2. Data and methods

We use the fully online coupled WRF-Chem model version 3.5.1, which permits the aerosol radiative forcing to affect the meteorology quantities and concentrations of air pollutants (Fast et al., 2006; Gao et al., 2016a). Model vertical resolution is 28 sigma-pressure levels and horizontal resolution is 60 km × 60 km. The modeling domain is shown in Fig. 1. The CBM-Z (Zaveri and Peters, 1999) photochemical mechanism coupled with the 8 sectional bin aerosol module, MOSAIC (Zaveri et al., 2008), is used to simulate gas phase and aerosol evolutions. Aerosols in MOSAIC are composed of sulfate, nitrate, ammonium, chloride, sodium, organic matter, black carbon, other inorganics (mostly dust), and some optional species such as calcium and carbonate (Zaveri et al., 2008). The Secondary Organic Aerosol (SOA) formation in MOSAIC was treated based on a computationally efficient scheme, Hodzic and Jimenez (2011), in which anthropogenic and biomass burning precursors are treated based on ambient aging measurements while biogenic SOA is treated as a two product approach using updated yields. Each aerosol constituent is associated with a complex index of refraction that represents its scattering and absorption properties, and optical properties are calculated using the Mie theory (Fast et al., 2006). Then the aerosol radiative properties are implemented in the shortwave/longwave radiative transfer model to calculate the direct aerosol forcing (Fast et al., 2006). In this study, the Rapid Radiative Transfer Method for Global (RRTMG) long-wave and short-wave radiation scheme is used (Iacono et al., 2008). Other configurations follow the settings in Gao et al. (2016a).

Anthropogenic emissions are taken from the MIX emission inventory (accessible at www.meicmodel.org), which combined five regional emission inventories, including the REAS v2.1 inventory for the entire Asia, the Tsinghua University MEIC inventory, the Peking University NH_3 emission inventory, the ANL India inventory and the

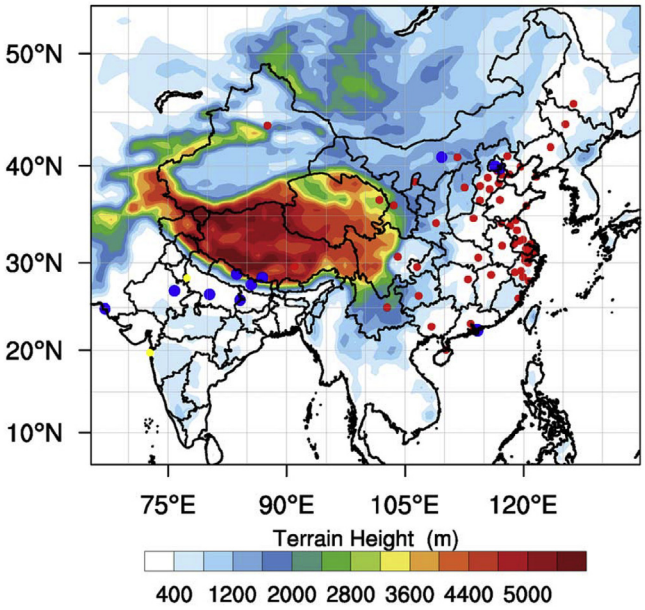

Fig. 1. The modeling domain and locations of used CNEMC (red dots), CPCB (yellow dots) and AERONET (blue dots) sites. (For interpretation of the references to colour in this figure legend, the reader is referred to the Web version of this article.)

official CAPSS inventory (Li et al., 2017). The emissions aggregated into five sectors (power, industry, residential, transportation, and agriculture) are provided at 0.25° × 0.25° spatial resolution and monthly temporal resolution for year 2008 and 2010 (Li et al., 2017). We use the 2010 inventory for this study. Biogenic emissions are calculated online using the MEGAN model (Guenther et al., 2006), and the biomass burning emissions are obtained from the GFED v4 database (Randerson et al., 2017). Wind-blown dust emissions are calculated online using the GOCART scheme (Ginoux et al., 2001). The NCEP FNL data is used as meteorological initial and boundary conditions. For chemical initial and boundary conditions, an idealized vertical profile based on climatological data from the NOAA Aeronomy Lab Regional Oxidant Model (NALROM) numerical chemistry model (McKeen et al., 1991) is employed.

A series of numerical experiments are conducted (Table 1) to investigate the sector contributions to aerosol radiative forcing, and each simulation covers the entire year of 2013. As described in Table 1, the differences between radiation fluxes from the CTL_{ARI_on} and the CTL_{ARI_off} simulations are used to calculate aerosol direct radiative forcing due to all sectors. The differences between radiation fluxes from the CTL_{ARI_on} and the $noIND_{ARI_on}$ simulations are used to compute

Table 1
Descriptions of numerical experiments.

Simulations	Descriptions
CTL_{ARI_on}	With all emissions included (anthropogenic, biogenic, biomass burning, and wind-blow dust), and aerosol-radiation interaction on
CTL_{ARI_off}	With all emissions included (anthropogenic, biogenic, biomass burning, and wind-blow dust), and aerosol-radiation interaction off
$noIND_{ARI_on}$	Same as CTL_{ARI_on}, except that industry emissions are excluded
$noPOW_{ARI_on}$	Same as CTL_{ARI_on}, except that power emissions are excluded
$noTRA_{ARI_on}$	Same as CTL_{ARI_on}, except that transportation emissions are excluded
$noRES_{ARI_on}$	Same as CTL_{ARI_on}, except that residential emissions are excluded
$noFIRE_{ARI_on}$	Same as CTL_{ARI_on}, except that fire emissions are excluded

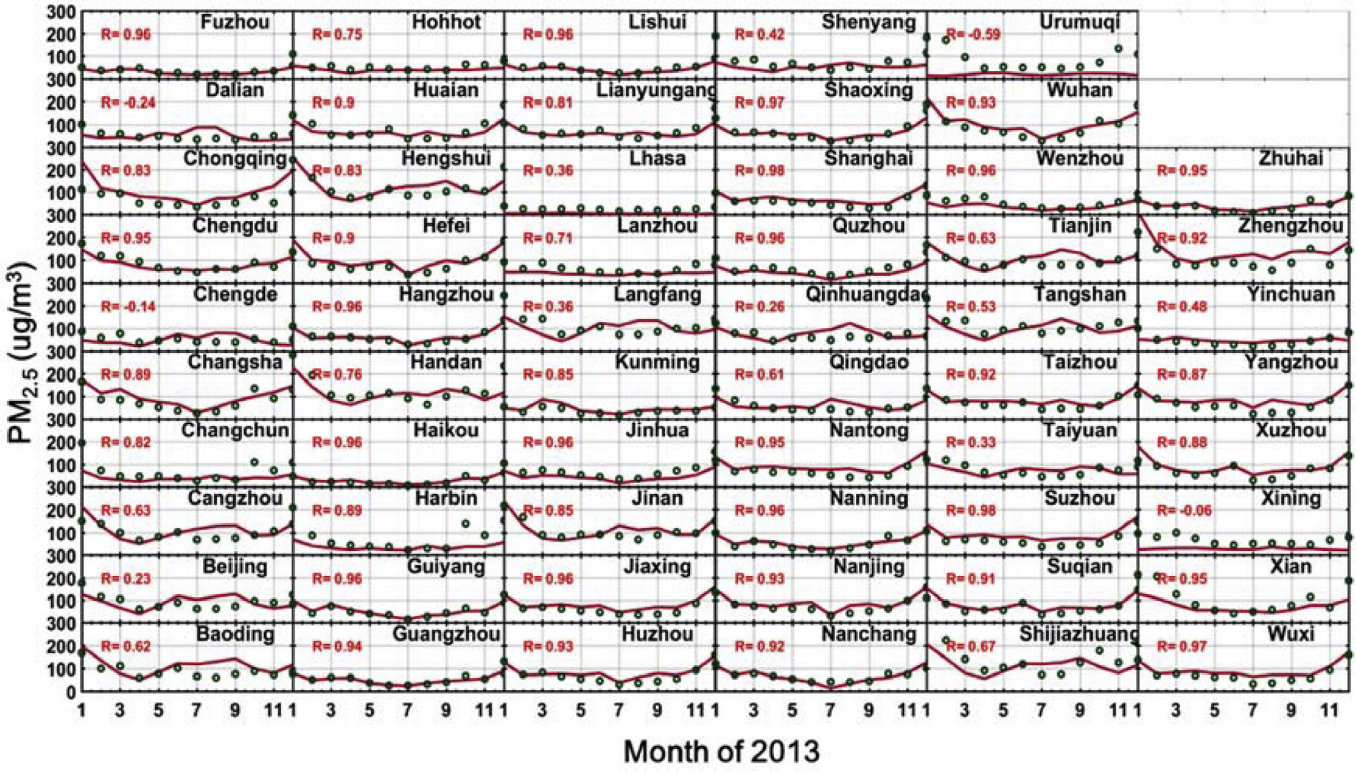

Fig. 2. Observed (green dots) monthly mean $PM_{2.5}$ concentrations and corresponding model (red line) simulation in the CNEMC sites. (For interpretation of the references to colour in this figure legend, the reader is referred to the Web version of this article.)

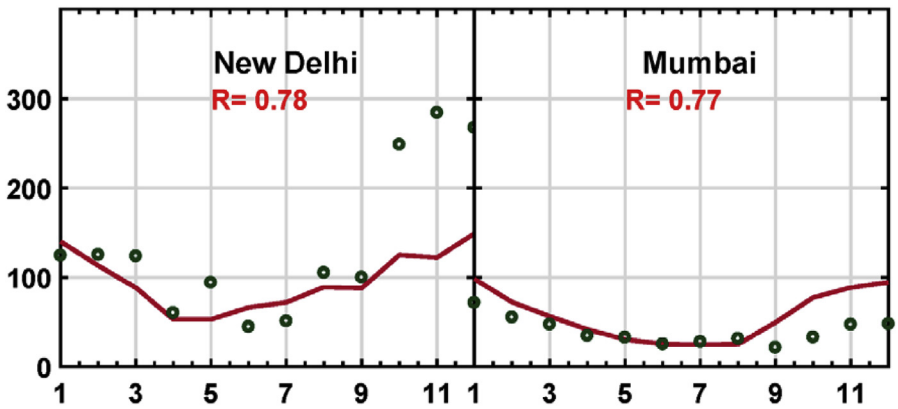

Fig. 3. Observed (green dots) monthly mean $PM_{2.5}$ concentrations and corresponding model (red line) simulation in the CPCB sites. (For interpretation of the references to colour in this figure legend, the reader is referred to the Web version of this article.)

the aerosol direct radiative forcing due to industry sector. The calculations for other sectors are similar.

3. Results and discussions

3.1. Model performance

We use multiple observations to validate our model performance in capturing temporal and spatial variations of aerosols, including the China nationwide surface $PM_{2.5}$ measurements, the Indian Central Pollution Control Board (CPCB) database, AERONET Aerosol Optical Depth (AOD) in both China and India, and $PM_{2.5}$ chemical compositions. The surface $PM_{2.5}$ measurements are available at the China National Environmental Monitoring Center website (CNEMC, http://www.cnemc.cn/). $PM_{2.5}$ chemical compositions were measured at the Institute of Atmospheric Physics, Chinese Academy of Sciences. The locations of the used CNEMC, CPCB, and AERONET sites are marked in red, yellow and blue in Fig. 1. Fig. 2 shows the monthly surface $PM_{2.5}$ concentrations in 2013 from the CNEMC network and the corresponding WRF-Chem simulation over the 48 cities across China. Arithmetic average of measured values within one model grid and then compared against the model value. In general, model results can reproduce the observed monthly variations and magnitudes for $PM_{2.5}$ over China. For most of the cities, the temporal correlation coefficient (R) values are higher than 0.8. In Suzhou and Shanghai, the R values can reach as high as 0.98. The calculated mean bias for all sites is $-2.05\ \mu g/m^3$ and the root mean square error is $27.00\ \mu g/m^3$, which are comparable to other model evaluation studies (Gao et al., 2018a). Poor performance is found in Urumuqi, which is likely caused by the errors in emissions (Ma et al., 2017). Overestimations of $PM_{2.5}$ during summer are shown in cities in North China, such as Beijing, Chengde, and Hengshui. Previous studies pointed out that the coarse resolution of

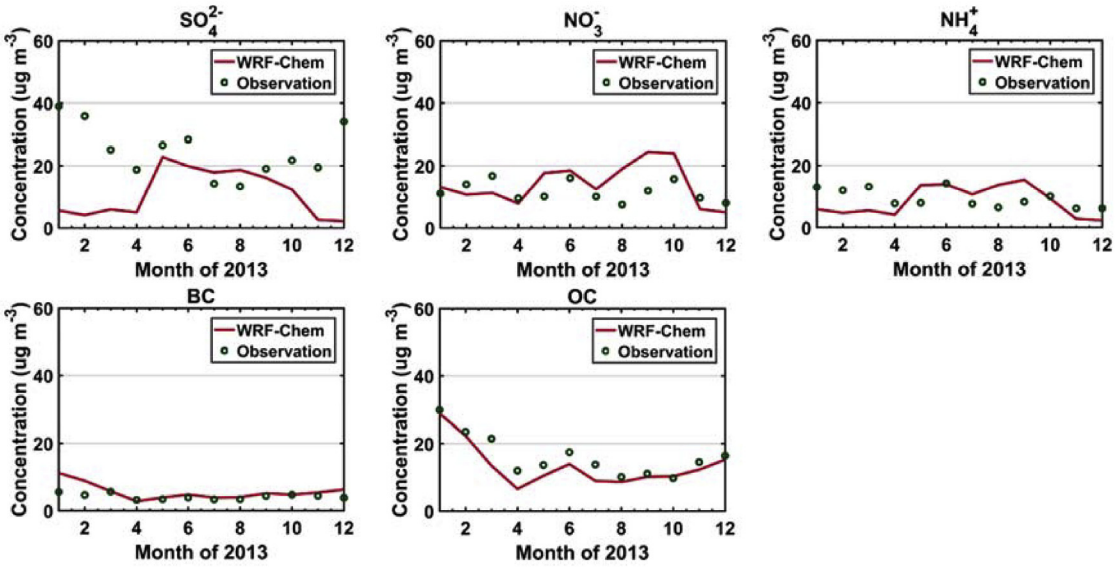

Fig. 4. Observed monthly mean concentrations of $PM_{2.5}$ components (sulfate, nitrate, ammonium, BC and OC) and corresponding model simulation in Beijing.

WRF modeling could lead to weaker rainfall and overestimation of air pollutants in North China (Lin et al., 2009). The magnitudes and variations of observed $PM_{2.5}$ concentrations in New Delhi and Mumbai are reproduced well by the model, except that extreme high $PM_{2.5}$ in winter in New Delhi is underestimated (Fig. 3). More comprehensive model evaluation of $PM_{2.5}$ concentrations across India can be found in Gao et al. (2018b).

Fig. 4 shows the comparison between WRF-Chem simulated and observed monthly mean sulfate, nitrate, ammonium, black carbon (BC), and organic carbon (OC) concentrations. Similar to many previous studies on winter haze formation (Gao et al., 2016a; Zheng et al., 2015), sulfate is underestimated by our model in winter months. It was proposed that aerosol dimming effects inhibited photochemical pathway of sulfate formation, and reactive nitrogen chemistry in aerosol water could explain the underestimation of sulfate during winter, which is missing in current models (Cheng et al., 2016; Gao et al., 2016b; Wang et al., 2016). The seasonal variation and magnitudes of nitrate is simulated well by the model. Ammonium is underestimated in winter months mainly due to the simulated low sulfate concentrations. The variation of BC is relatively flat, and high agreement between model and observation is found. OC concentrations are highest in January in Beijing because of high emissions from residential heating and stagnant weather conditions in winter (Gao et al., 2016b). Relatively lower OC concentrations are shown in spring and fall. In summer, OC concentrations are underestimated by the model, which is likely caused by model difficulty in capturing secondary organic aerosol formation (Gao et al., 2017).

Fig. 5 presents the observed daily mean aerosol optical depth (AOD) at 550 nm from AERONET and the corresponding model results. In North China (Beijing and Xianghe stations), the seasonal variation can be reproduced, but AOD is overestimated in summer. As mentioned above, the 60 km model resolution in this study might not be ideal to simulate cloud and rainfall during summer, which is likely to underestimate wet deposition (Lin et al., 2009). In coastal regions (HKPU and HKS sites in Hong Kong) and less developed regions (Baotou city) in China, the simulated AOD values show better consistency with measurements, with much lower magnitudes than in North China. The observed AOD in Southeast Asia is generally lower than in China, but similar overestimations during summer are also found. The correlation coefficients between model and observations range from 0.22 to 0.94 for sites in China, and range from 0.31 to 0.45 for sites in India, which are comparable to previous model evaluation studies (Gao et al., 2014).

3.2. Sectoral contribution

Table 2 presents the disaggregation of emissions in China and India into major sectors for year 2010 (Li et al., 2017). Large amounts of BC and OC were emitted from the residential and industry sectors, but negligible amounts were produced by power sector. SO_2 and NO_x play the dominant roles in secondary inorganic aerosol formation, which primarily come from industry and power sectors. In India, transportation sector emitted more NO_x than power sector. Fig. 6 shows the aerosol direct radiative forcing (both shortwave and longwave) associated with emitting sectors in China and India. The corresponding changes in near surface temperature are presented in Fig. S1 in the supplementary material. The aerosol direct radiative forcing due to all sectors are negative with China national mean of $-2.21\ W/m^2$ and India national mean of $-3.18\ W/m^2$. Enhanced values are shown in the Sichuan Basin region in China and East India region. The largest forcing can reach $-8\ W/m^2$. Unlike the evenly distributed forcing in India, high values of aerosol forcing in China are mainly located in East China, corresponding to the severe aerosol pollution there. The negative aerosol forcing in both China and India is dominated by the power sector because of its large contribution to emissions of sulfate and nitrate precursors. Given the underprediction of sulfate and nitrate in the model (Fig. 4), the power sector radiative forcing might have been underestimated here. In addition, power sector shows insignificant contribution to BC emissions, which heat the atmosphere. In China, the contribution from the transportation and biomass burning sectors are minor. In India, the role of industry and biomass burning sectors are unimportant. Industry is the second largest sector contributing to negative forcing in China, while transportation is the second largest sector contributing to negative forcing in India due to their appreciated share in SO_2 and NO_x emissions. In both China and India, the residential sector leads to positive aerosol forcing because of its dominant contribution to BC emissions and relatively less emissions of SO_2 and NO_x. Accordingly, residential sector would be an effective target for reducing global warming. If emissions from residential were eliminated, the radiative forcing would be reduced by 0.97 and $2.39\ W/m^2$ in China and India, respectively. Although there is scattering components from residential sector, the strong absorption from BC is sufficient to cancel the negative forcing of sulfate, nitrate and OC. It would be even more effective by targeting subsectors that have relatively larger BC emissions relative to scattering components, such as diesel (Koch et al., 2007b). The importance of biomass burning in aerosol forcing is limited only in

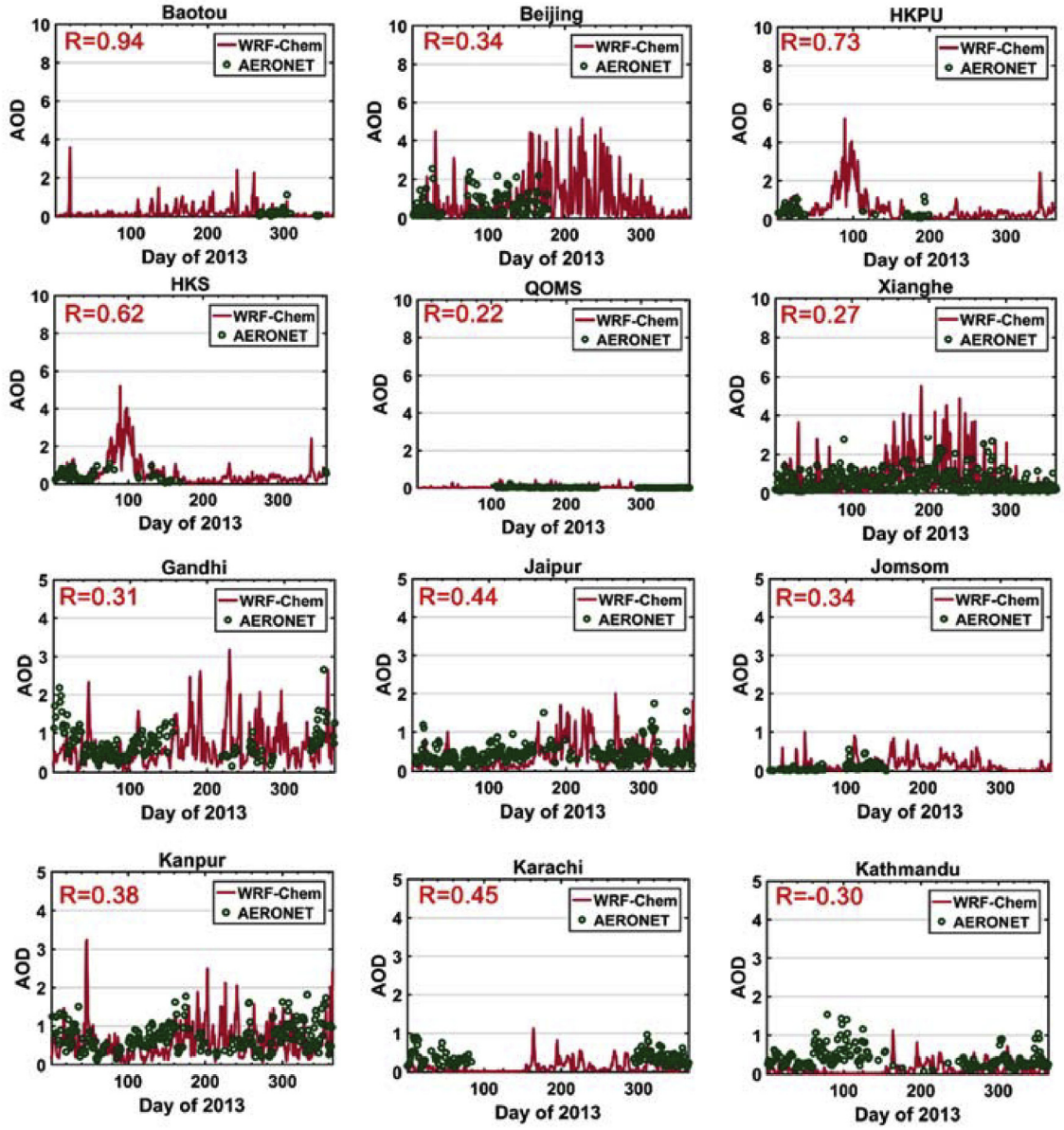

Fig. 5. Observed daily mean AOD in the AERONET sites and corresponding model simulation in Beijing.

Table 2
Aerosol emissions: sectoral contributions.

	BC		OC		SO_2		NO_x	
	China	India	China	India	China	India	China	India
Industry	575	217	530	200	16775	2959	11218	973
Residential	908	709	2752	2275	3489	685	1140	968
Power	2	1	0	3	8166	5476	9455	2391
Transport	281	92	104	52	234	139	7257	5233

South China and East India, leading to smaller contribution to national mean aerosol radiative forcing. It was found that warming over the Arctic is more rapid than other regions, which could be partially caused by the long range transported black carbon (Koch and Hansen, 2005). Model results suggest that the predominant sources of Arctic black carbon are from South Asia (Koch and Hansen, 2005). Thus, reduced residential emissions would not only benefit regional climate, but global climate as well.

3.3. Subdivision and seasonality

Fig. 7 shows the subdivisions of aerosol direct radiative forcing into shortwave and longwave forcing for each emitting sector. Consistent with Reddy et al. (2005), the longwave radiative forcing is generally positive and slightly offsets the negative shortwave forcing for biomass, transportation, power and industry sectors. Reddy et al. (2005) argued that longwave radiative forcing are mainly exerted by coarse-mode aerosols, such as dust. As shown in Fig. 6, enhanced longwave radiative forcing are attributed to residential, industry and power sectors, which dominate emissions of coarse-mode primary particles (PM_{10}) (Li et al., 2017). As pointed out in the most recent IPCC report (Pachauri et al., 2014), estimates of aerosol longwave radiative forcing remain limited. In this study, we report that the national mean longwave radiative forcing due to all sectors is approximately 0.86 W/m^2 for China and 1.21 W/m^2 for India. For anthropogenic sectors, longwave forcing is dominantly contributed by residential, power and industry sectors.

We now consider the seasonality of the sectoral aerosol forcing for China and India. As shown in Fig. 7, sectoral aerosol direct forcing exhibit distinct seasonality, roughly with maximum in summer and

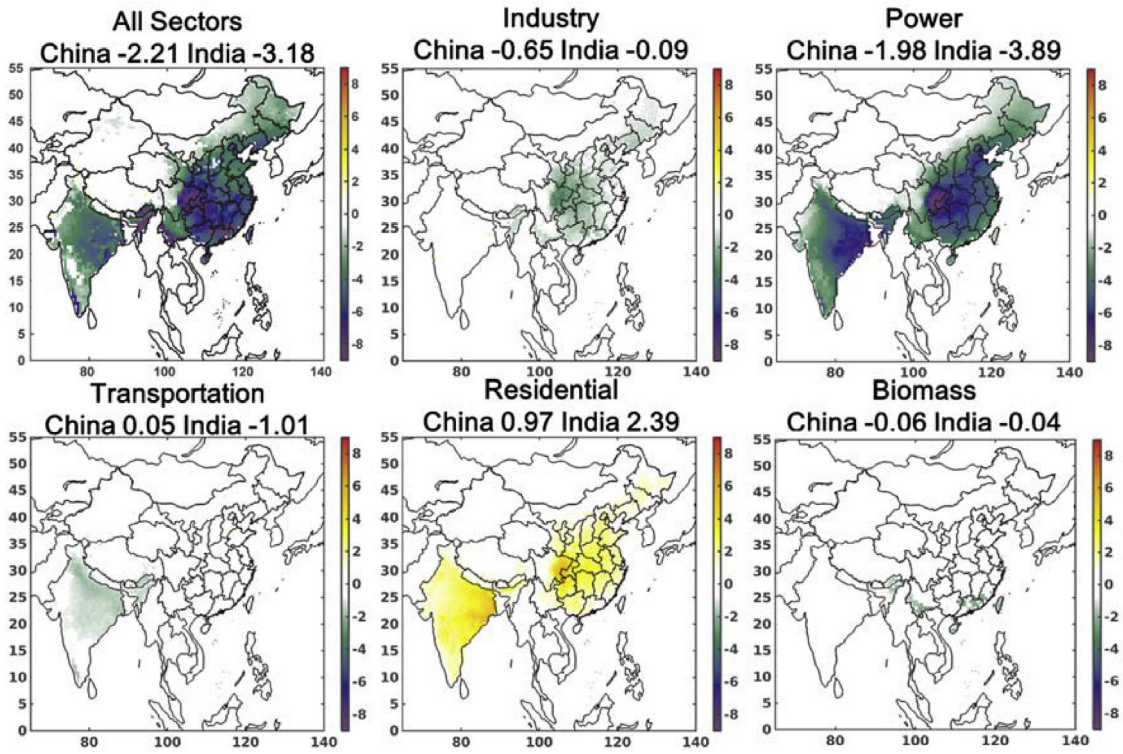

Fig. 6. Aerosol direct radiative forcing due to all sectors, industry sector, power sector, transportation sector, residential sector and biomass burning sector.

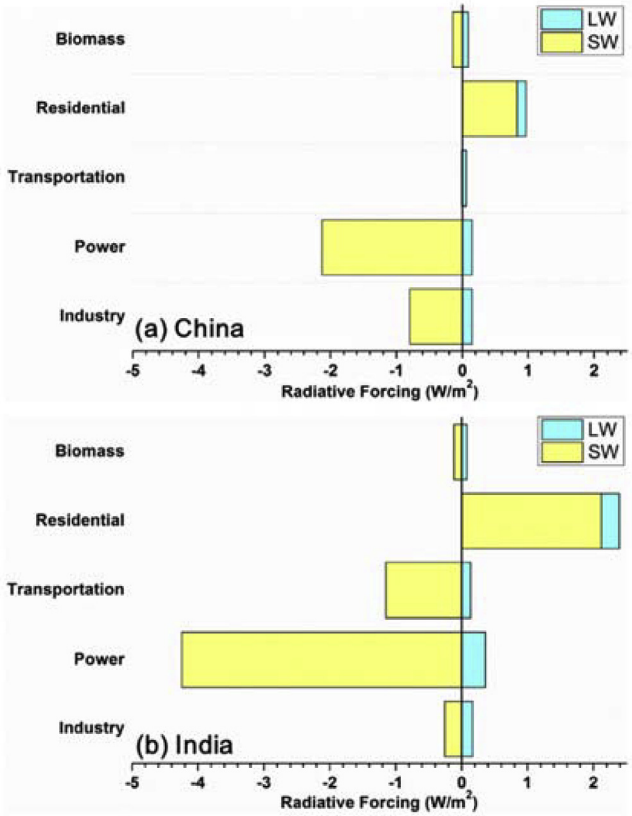

Fig. 7. National mean aerosol direct longwave and shortwave radiative forcing for China and India.

minimum in winter for China, which is consistent with the results presented in Huang et al. (2015). However, the seasonality of residential sector induced forcing greatly differ, with largest value in winter and lowest value in fall. In China, residential emissions peak in winter due to heating. Because of the lower latitude, the seasonality of residential emissions in India differs from it in China. For India, the power and transportation sectors induced forcing show maximum in fall and minimum in spring. The differences between the seasonality in China and India are very likely caused by the removal processes during the Indian summer monsoon season (Lu et al., 2018). The severely polluted North China region is less influenced by summer monsoon compared to South China region, while the India subcontinent is largely affected by the Indian Summer Monsoon (Ding and Chan, 2005). As indicated by the seasonal measurements of $PM_{2.5}$ and BC in India, concentrations were lower in monsoon season compared with other seasons (Tiwari et al., 2013).

3.4. Comparisons with other studies

Although studies on sector contribution to local/regional aerosol radiative forcing in China and India are limited, there have been several studies evaluating aerosol direct radiative forcing over China or Asia region. In this study, we estimate the clear sky aerosol radiative forcing is $-2.21\ W/m^2$ over China. We compare this estimation with other existing studies. Chung et al. (2010) compared anthropogenic aerosol radiative forcing averaged over the INDOEX domain (40–100°E and Equator-20°N) for the January–March period. Their estimates using aerosol data assimilation is $-3.6\ W/m^2$ (Chung et al., 2010), which is larger their previous estimate of $-2.9\ W/m^2$ (Chung et al., 2005) and the value derived from the NCAR/CCSM3 model ($-1.1\ W/m^2$). Gao et al. (2014) concluded that the clear sky anthropogenic aerosol forcing for the region of 70–150°E and 10–50.5°N is about $-3.7\ W/m^2$. Gao et al. (2017) applied an aerosol data assimilation system to reduce uncertainties in aerosol forcing estimates in North China in January 2013 and found high aerosol loadings in winter in North China led to a negative forcing of $-2.9\ W/m^2$. Although different domains are used to calculate the mean forcing, our estimate is generally in line with these estimates. Another estimation based on average within China borders

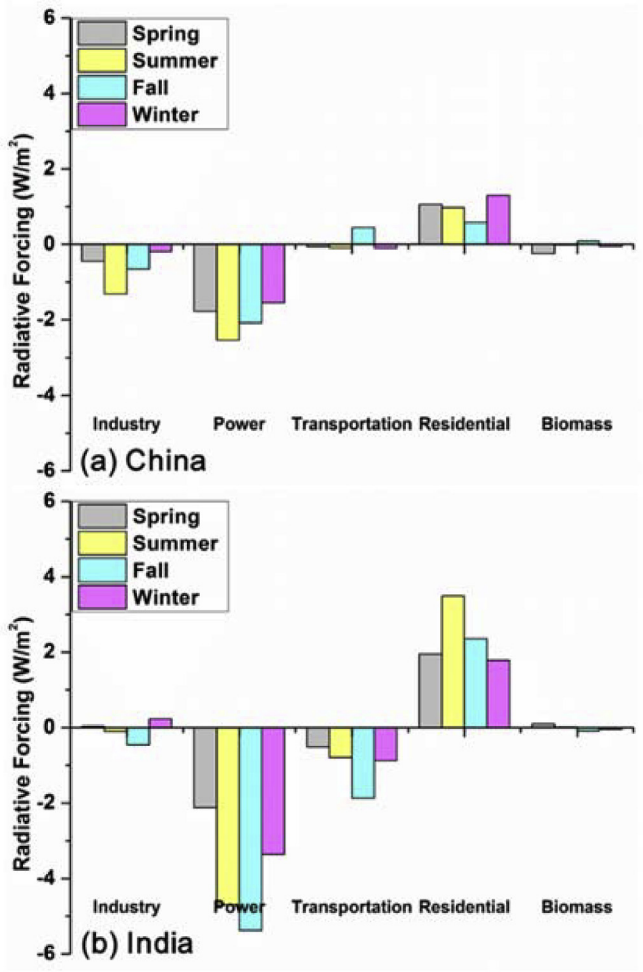

Fig. 8. Seasonal variations in national mean sectoral aerosol direct radiative forcing for China and India.

concluded that all aerosols resulted in $+0.6$ W/m^2 over China for the year 2006 (Huang et al., 2015), emphasizing the heating effects of BC over China.

4. Summary

Using a fully online coupled meteorology-chemistry model, we estimate the direct aerosol radiative forcing over China and India, and the attributions to different emitting sectors. Model simulations were validated with multiple observational datasets, including nation-wide surface $PM_{2.5}$ measurements in China, aerosol compositions in Beijing, and ground-based AOD observations in both China and India. In general, high consistency between model and measurements are found. However, high sulfate concentrations are still underestimated in winter months, which is likely caused by missing aqueous and/or heterogeneous chemistry in the model.

Aerosols from all sectors resulted in negative forcing at the TOA over China (-2.21 W/m^2) and India (-3.18 W/m^2), with the largest contribution from power sector. The contribution of the emissions from the power sector in China is followed in magnitude by the forcing from the industrial sector and then by the transportation sector in India. Residential sector leads to positive forcing over both China and India. These results indicate that controlling residential sector would be more effective to benefit both air quality and climate change. The subdivision of longwave and shortwave forcing show that the energy balance is dominated by shortwave forcing, and longwave forcing is largely induced by sectors that emit coarse-mode particles (see Fig. 8).

The seasonal characteristics of sectoral aerosol forcing for China and India are different. For China, negative forcing dominant sectors (power and industry sectors) show a maximum in summer due to hygroscopic growth and incident radiation flux, while positive forcing sector (residential sector) exhibits a maximum in winter due to emissions from residential heating. For India, the seasonality of sectoral radiative forcing is modulated by the Indian Summer Monsson, and thus shows relatively lower values in summer. Our estimates of aerosol forcing in Asia are in good agreements with previous studies in the same region, but provide additional sectoral information, which is critical for synergic control benefits for both air pollution and climate change.

Although a sophisticated regional meteorology-chemistry model, a state-of-the-art emission inventory in Asia, and multiple observations were used in this study to constrain the estimates of aerosol direct radiative forcing in China and India, with sectoral information, there are still a number of limitations within this study, involving different aspects of the calculations. (1) Model evaluation of aerosol components was conducted only in Beijing. The model capability of simulating aerosol compositions are of great importance for radiative forcing estimates, but the accuracy of model aerosol composition, particularly in India, are uncertain due to lack of widespread measurements of aerosol compositions. (2) The uncertainty in emission inventory is particularly large over India. Given the underestimation of aerosol concentrations during winter in Delhi, the aerosol radiative forcing might have been underpredicted over that region. (3) In this study, only direct radiative forcing is considered, as tremendous uncertainties still remain in the parameterization of indirect aerosol effects in models. Considering the large computational needs within current study, we use a relatively coarse resolution (60 km), which is not good for simulations of clouds and precipitation. The indirect radiative forcing of aerosols might change the conclusion in this study. The model physical settings follows Gao et al. (2016a), and future investigation on indirect radiative forcing are necessary with finer model configurations. (4) Current policy implications are solely based on sector contributions to aerosol direct radiative forcing, with unknown information on the indirect forcing. Thus, the conclusions should be referenced with caution.

Acknowledgement

We thank the AERONET measurement groups for establishing and maintaining the AERONET sites used in this study. The aerosol composition measurements used in this study was supported by the Ministry of Science and Technology of China (2016YFC0202701), and the Beijing Municipal Science and Technology Project (D17110900150000; Z171100000617002).

Appendix A. Supplementary data

Supplementary data related to this article can be found at https://doi.org/10.1016/j.atmosenv.2018.07.011.

References

Cheng, Yafang, Zheng, Guangjie, Wei, Chao, Mu, Qing, Zheng, Bo, Wang, Zhibin, Gao, Meng, et al., 2016. Reactive nitrogen chemistry in aerosol water as a source of sulfate during haze events in China. Sci. Adv. 2 (12), e1601530.

Chung, Chul Eddy, Ramanathan, V., Kim, Dohyeong, Podgorny, I.A., 2005. Global anthropogenic aerosol direct forcing derived from satellite and ground-based observations. J. Geophys. Res. Atmos. 110 (D24).

Chung, Chul Eddy, Ramanathan, V., Carmichael, Gregory, Kulkarni, S., Tang, Youhua, Adhikary, Bhupesh, Leung, L.R., Qian, Yun, 2010. Anthropogenic aerosol radiative forcing in Asia derived from regional models with atmospheric and aerosol data assimilation. Atmos. Chem. Phys. 10 (13), 6007–6024.

Dang, H., Unger, N., 2015. Contrasting regional versus global radiative forcing by megacity pollution emissions. Atmos. Environ. 119, 322–329.

Ding, Yihui, Chan, Johnny CL., 2005. The East Asian summer monsoon: an overview. Meteorol. Atmos. Phys. 89 (1–4), 117–142.

Fast, J.D., Gustafson, W.I., Easter, R.C., Zaveri, R.A., Barnard, J.C., Chapman, E.G., Grell, G.A., Peckham, S.E., 2006. Evolution of ozone, particulates, and aerosol direct

radiative forcing in the vicinity of Houston using a fully coupled meteorology-chemistry-aerosol model. J. Geophys. Res. Atmos. 111 (D21).
Gao, Yi, Chun, Zhao, Liu, Xiaohong, Zhang, Meigen, Ruby Leung, L., 2014. WRF-Chem simulations of aerosols and anthropogenic aerosol radiative forcing in East Asia. Atmos. Environ. 92, 250–266.
Gao, M., Carmichael, G.R., Wang, Y., Saide, P.E., Yu, M., Xin, J., Liu, Z., Wang, Z., 2016a. Modeling study of the 2010 regional haze event in the North China Plain. Atmos. Chem. Phys. 16 (3).
Gao, Meng, Carmichael, Gregory R., Wang, Yuesi, Ji, Dongsheng, Liu, Zirui, Wang, Zifa, 2016b. Improving simulations of sulfate aerosols during winter haze over Northern China: the impacts of heterogeneous oxidation by NO_2. Front. Environ. Sci. Eng. 10 (5), 16.
Gao, Meng, Saide, Pablo E., Xin, Jinyuan, Wang, Yuesi, Liu, Zirui, Wang, Yuxuan, Wang, Zifa, Pagowski, Mariusz, Guttikunda, Sarath K., Carmichael, Gregory R., 2017. Estimates of health impacts and radiative forcing in winter haze in eastern China through constraints of surface $PM_{2.5}$ predictions. Environ. Sci. Technol. 51 (4), 2178–2185.
Gao, Meng, Han, Zhiwei, Liu, Zirui, Li, Meng, Xin, Jinyuan, Tao, Zhining, Li, Jiawei, et al., 2018a. Air quality and climate change, topic 3 of the model inter-comparison study for Asia phase III (MICS-Asia III)–Part 1: overview and model evaluation. Atmos. Chem. Phys. 18 (7), 4859.
Gao, M., Beig, G., Song, S., Zhang, H., Hu, J., Ying, Q., Liang, F., Liu, Y., Wang, H., Lu, X., Zhu, T., Carmichael, G.R., Nielsen, C.P., McElroy, M.B., 2018b. The impact of power generation emissions on ambient $PM_{2.5}$ pollution and human health in China and India. Environ. Int Submitted.
Ginoux, P., Chin, M., Tegen, I., Prospero, J., Holben, B., Dubovik, O., Lin, S.-J., 2001. Sources and global distributions of dust aerosols simulated with the GOCART model. J. Geophys. Res. 106, 20,255–20,273.
Guenther, A., Karl, T., Harley, P., Wiedinmyer, C., Palmer, P.I., Geron, C., 2006. Estimates of global terrestrial isoprene emissions using MEGAN (model of emissions of gases and aerosols from nature). Atmos. Chem. Phys. 6 (11), 3181–3210.
Hodzic, A., Jimenez, J.L., 2011. Modeling anthropogenically controlled secondary organic aerosols in a megacity: a simplified framework for global and climate models. Geosci. Model Dev. 4 (4), 901–917.
Huang, Xin, Song, Yu, Zhao, Chun, Cai, Xuhui, Zhang, Hongsheng, Zhu, Tong, 2015. Direct radiative effect by multicomponent aerosol over China. J. Clim. 28 (9), 3472–3495.
Iacono, Michael J., Delamere, Jennifer S., Mlawer, Eli J., Shephard, Mark W., Clough, Shepard A., Collins, William D., 2008. Radiative forcing by long-lived greenhouse gases: calculations with the AER radiative transfer models. J. Geophys. Res. Atmos. 113 (D13).
Koch, Dorothy, Hansen, James, 2005. Distant origins of arctic black carbon: a Goddard Institute for space studies ModelE experiment. J. Geophys. Res. Atmos. 110 (D4).
Koch, Dorothy, Bond, Tami C., Streets, David, Unger, Nadine, 2007a. Linking future aerosol radiative forcing to shifts in source activities. Geophys. Res. Lett. 34 (5).
Koch, Dorothy, Bond, Tami C., Streets, David, Unger, Nadine, Van der Werf, Guido R., 2007b. Global impacts of aerosols from particular source regions and sectors. J. Geophys. Res. Atmos. 112 (D2).
Li, Meng, Zhang, Qiang, Kurokawa, Jun-ichi, Woo, Jung-Hun, He, Kebin, Lu, Zifeng, Ohara, Toshimasa, et al., 2017. MIX: a mosaic Asian anthropogenic emission inventory under the international collaboration framework of the MICS-Asia and HTAP. Atmos. Chem. Phys. 17 (2), 935.
Lin, M., Holloway, T., Oki, T., Streets, D.G., Richter, A., 2009. Multi-scale model analysis of boundary layer ozone over East Asia. Atmos. Chem. Phys. 9 (10).
Lu, X., Zhang, L., Liu, X., Gao, M., Zhao, Y., Shao, J., 2018. Lower tropospheric ozone over India and its linkage to the South Asian monsoon. Atmos. Chem. Phys. 18, 3101–3118.
Ma, Q., Cai, S., Wang, S., Zhao, B., Martin, R.V., Brauer, M., Cohen, A., Jiang, J., Zhou, W., Hao, J., Frostad, J., 2017. Impacts of coal burning on ambient $PM_{2.5}$ pollution in China. Atmos. Chem. Phys. 17 (7), 4477–4491.
McKeen, S.A., Hsie, E.-Y., Liu, S.C., 1991. A study of the dependence of rural ozone on ozone precursors in the eastern United States. J. Geophys. Res. Atmos. 96 (D8), 15377–15394.
Menon, S., Hansen, J., Nazarenko, L., Luo, Y., 2002. Climate effects of black carbon aerosols in China and India. Science 297 (5590), 2250–2253.
Pachauri, Rajendra K., Allen, Myles R., Barros, Vicente R., Broome, John, Cramer, Wolfgang, Christ, Renate, Church, John A., et al., 2014. Climate Change 2014: Synthesis Report. Contribution of Working Groups I, II and III to the fifth assessment report of the Intergovernmental Panel on Climate Change. IPCC.
Qian, Y., Giorgi, F., 2000. Regional climatic effects of anthropogenic aerosols? The case of Southwestern China. Geophys. Res. Lett. 27 (21), 3521–3524.
Ramanathan, V., Carmichael, G., 2008. Global and regional climate changes due to black carbon. Nat. Geosci. 1 (4), 221.
Randerson, J.T., van der Werf, G.R., Giglio, L., Collatz, G.J., Kasibhatla, P.S., 2017. Global Fire Emissions Database, Version 4.1 (GFEDv4). ORNL DAAC, Oak Ridge, Tennessee, USA. https://doi.org/10.3334/ORNLDAAC/1293.
Reddy, M. Shekar, Boucher, Olivier, Balkanski, Yves, Schulz, Michael, 2005. Aerosol optical depths and direct radiative perturbations by species and source type. Geophys. Res. Lett. 32 (12).
Schmidt, G.A., Ruedy, R., Hansen, J.E., Aleinov, I., Bell, N., Bauer, M., Bauer, S., Cairns, B., Canuto, V., Cheng, Y., Del Genio, A., 2006. Present-day atmospheric simulations using GISS ModelE: comparison to in situ, satellite, and reanalysis data. J. Clim. 19 (2), 153–192.
Shindell, D., Lamarque, J.-F., Unger, N., Koch, D., Faluvegi, G., Bauer, S., Ammann, M., Cofala, J., Teich, H., 2008. Climate forcing and air quality change due to regional emissions reductions by economic sector. Atmos. Chem. Phys. 8 (23), 7101–7113.
Stohl, A., Aamaas, B., Amann, M., Baker, L.H., Bellouin, N., Berntsen, T.K., Boucher, O., Cherian, R., Collins, W., Daskalakis, N., Dusinska, M., 2015. Evaluating the climate and air quality impacts of short-lived pollutants. Atmos. Chem. Phys. 15 (18), 10529–10566.
Streets, David G., Shindell, Drew T., Lu, Zifeng, Faluvegi, Greg, 2013. Radiative forcing due to major aerosol emitting sectors in China and India. Geophys. Res. Lett. 40 (16), 4409–4414.
Tiwari, S., Srivastava, A.K., Bisht, D.S., Parmita, P., Srivastava, Manoj K., Attri, S.D., 2013. Diurnal and seasonal variations of black carbon and $PM_{2.5}$ over New Delhi, India: influence of meteorology. Atmos. Res. 125, 50–62.
Unger, Nadine, 2012. Global climate forcing by criteria air pollutants. Annu. Rev. Environ. Resour. 37, 1–24.
Unger, Nadine, Shindell, Drew T., Koch, Dorothy M., Streets, David G., 2008. Air pollution radiative forcing from specific emissions sectors at 2030. J. Geophys. Res. Atmos. 113 (D2).
Unger, Nadine, Shindell, Drew T., Wang, James S., 2009. Climate forcing by the on-road transportation and power generation sectors. Atmos. Environ. 43 (19), 3077–3085.
Unger, Nadine, Bond, Tami C., Wang, James S., Koch, Dorothy M., Menon, Surabi, Shindell, Drew T., Bauer, Susanne, 2010. Attribution of climate forcing to economic sectors. Proc. Natl. Acad. Sci. 107 (8), 3382–3387.
Unger, Nadine, Zhao, Yupu, Dang, Hongyan, 2013. Mid-21st century chemical forcing of climate by the civil aviation sector. Geophys. Res. Lett. 40 (3), 641–645.
Wang, Gehui, Zhang, Renyi, Gomez, Mario E., Yang, Lingxiao, Levy Zamora, Misti, Hu, Min, Lin, Yun, et al., 2016. Persistent sulfate formation from London Fog to Chinese haze. Proc. Natl. Acad. Sci. 113 (48), 13630–13635.
Yu, H., Kaufman, Y.J., Chin, M., Feingold, G., Remer, L.A., Anderson, T.L., Balkanski, Y., et al., 2006. A review of measurement-based assessments of the aerosol direct radiative effect and forcing. Atmos. Chem. Phys. 6 (3), 613–666.
Zaveri, Rahul A., Peters, Leonard K., 1999. A new lumped structure photochemical mechanism for large-scale applications. J. Geophys. Res. Atmos. 104 (D23), 30387–30415.
Zaveri, Rahul A., Easter, Richard C., Fast, Jerome D., Peters, Leonard K., 2008. Model for simulating aerosol interactions and chemistry (MOSAIC). J. Geophys. Res. Atmos. 113 (D13).
Zheng, Bo, Zhang, Qiang, Zhang, Yang, He, K.B., Wang, K., Zheng, G.J., Duan, F.K., Ma, Y.L., Kimoto, T., 2015. Heterogeneous chemistry: a mechanism missing in current models to explain secondary inorganic aerosol formation during the January 2013 haze episode in North China. Atmos. Chem. Phys. 15 (4), 2031.